

### 4.1 Grinding of low carbon steel

The upcoming subsection reports the grindability of low carbon steel in terms of grinding forces, specific grinding energy, grinding temperature and surface integrity. The measurement of above grindability indices is important in order to understand the correlation between surface integrity and the associated change in micromagnetic response.

#### 4.1.1 Grinding forces:

Forces generated during grinding operation contribute significantly to the finished product. They play a major role in determining the surface finish, part dimensions of the ground workpiece, and cycle times of the grinding operation (Brach *et al.*, 1988; Koji, 1961). Interaction between wheel and the workpiece during grinding results into generation of normal grinding force, tangential grinding force and a component force in the direction of longitudinal feed. However, force acting in the longitudinal feed direction has no significance in the grinding operation and are not measured usually.

Fig.4.1 shows the variation in tangential grinding force ( $F_T$ ) with downfeed under different work velocity (8m/min & 12m/min) and grinding environment (dry & wet). The increase in downfeed result into increase in tangential grinding force. This is due to, increase in downfeed increases the effective number of grit as well as contact length. In other words, increase in downfeed increases the chip load and thus tangential grinding force. The maximum uncut chip thickness ( $h_{max}$ ) is related with table feed in

## Chapter 4 | Results and Discussion

accordance with eqn (4.1). It is clear that ( $h_{max}$ ) increases with increase in work velocity which thus expectedly increase the grinding force.

$$h_{max} = \left( \frac{2}{\rho_g \tan \alpha} \frac{V_w}{V_s} \sqrt{\frac{a}{d_g}} \right)^{\frac{1}{2}} \quad (\text{Malkin, 1989}) \quad (4.1)$$

Where,  $\rho_g$  - alumina abrasive grit density,  $\alpha$  - effective negative rake angle of abrasive grit,  $d_g$  - diameter of grinding wheel,  $v_w$  – work velocity and  $v_s$  -wheel speed,  $a$  - downfeed.

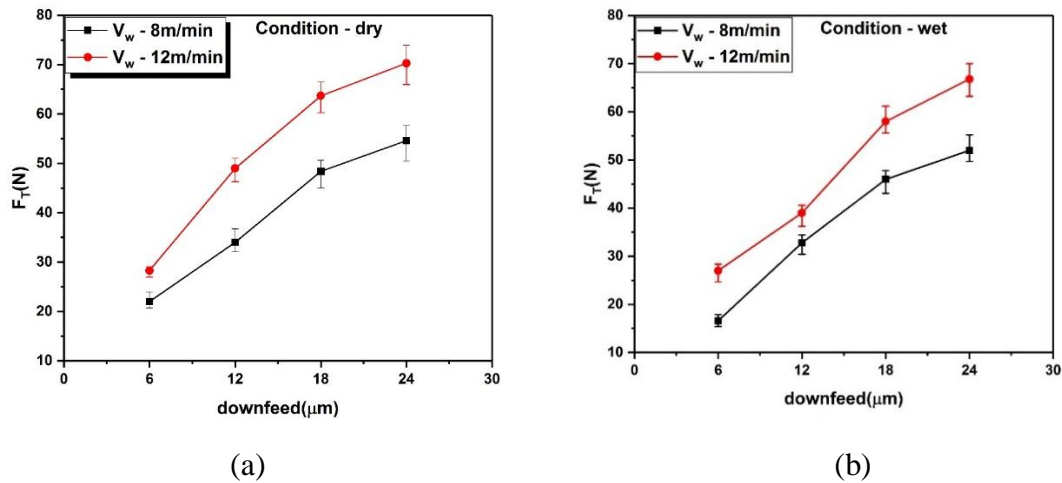


Fig.4.1 Variation in tangential grinding forces with downfeed under different work velocity conditions for (a) dry grinding (b) wet grinding

In wet grinding, the presence of cutting fluid helps in cleaning away the microchips formed during the process of shearing, thereby it reduces the chip load and consequently result into smaller grinding force. However, during dry grinding in the absence of cutting fluid chip load increases and thereby leads to higher grinding force. Similar to tangential grinding force, normal forces ( $F_N$ ) during grinding also increases with increase in downfeed and work velocity as can be seen from Fig.4.2.

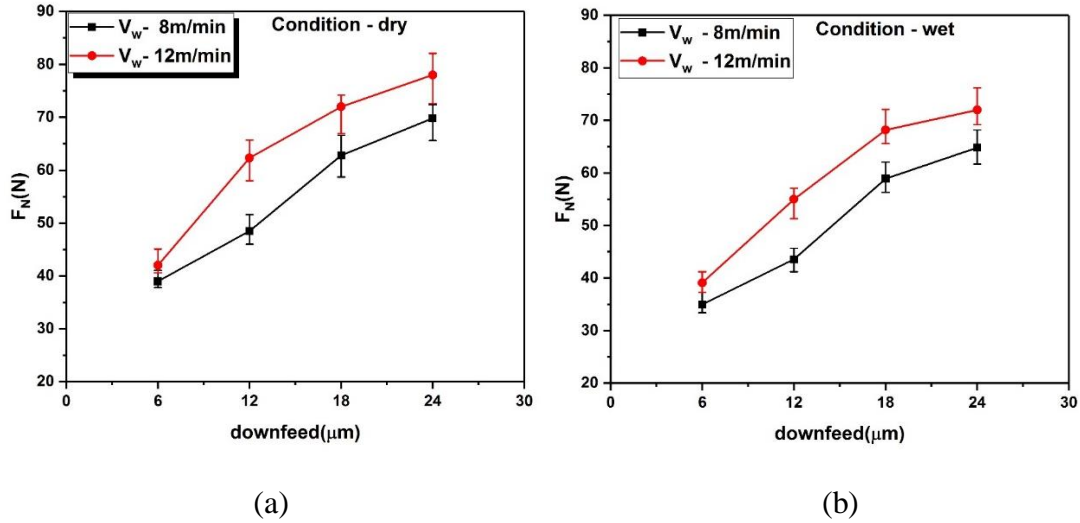


Fig.4.2 Variation in normal grinding forces with downfeed under different work velocity conditions for (a) dry grinding (b) wet grinding

The grinding environment, wet grinding also reduces the value of normal grinding forces comparative to dry grinding. This similar behavior of grinding forces is due to the fact that both are the function of chip load.

#### 4.1.2 Specific grinding energy:

Specific grinding energy is characterized by energy spent in removing unit volume of material. A low specific energy process is rather considered as a more environmental friendly technique. However, specific energy consumed during grinding is nearly two fold as compared to those of metal cutting operation. During deformation very small size grinding chips have proportionally greater strength as compared to large ones as a result extremely high dislocation densities occur in the shear zone, thereby increasing the grinding energy also higher specific energy is due to energy spent in undesirable rubbing and ploughing mechanism. Specific energy in grinding is estimated by eqn (3.1)

## Chapter 4 | Results and Discussion

The nature of specific grinding energy with downfeed, work velocity and grinding environment is as shown in Fig.4.3. It can be noted that specific energy decreases with increase in downfeed as well as work velocity. In the presence of coolant specific energy further decreases in comparison to dry grinding as the presence of coolant decreases the tangential grinding force and hence reducing the specific energy. The decrease in specific energy with increase in downfeed is attributed to the reason that, with increase in downfeed, maximum uncut chip thickness ( $h_{max}$ ) increases this in turn reduces the average effective negative rake angle of the abrasive grit thereby reducing the undesirable rubbing and ploughing action during chip formation and facilitates more cutting action.

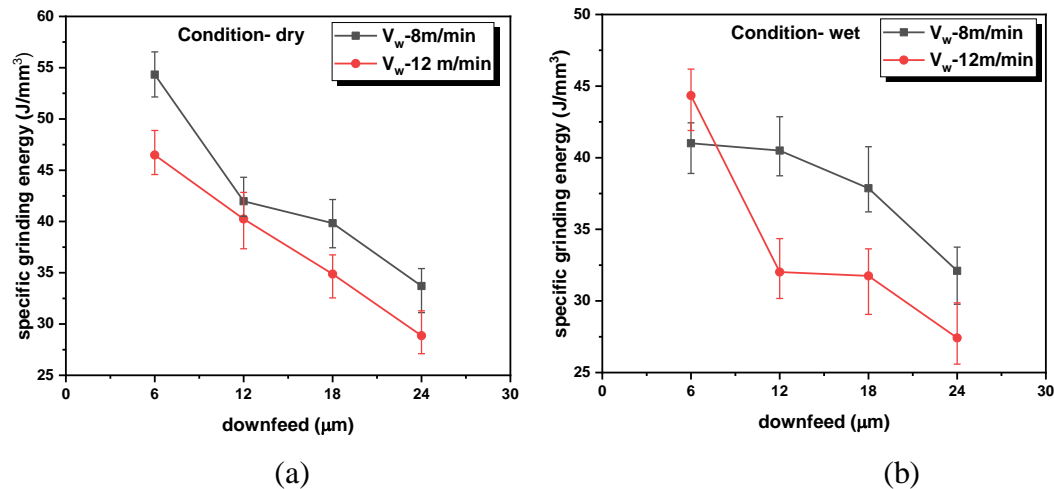


Fig.4.3 Variation of specific grinding energy with downfeed under different work velocity conditions (a) dry grinding (b) wet grinding

### 4.1.3 Grinding temperature:

The high temperature in grinding is the consequence of high specific grinding energy, as major proportion of this is converted into heat and get concentrated into grinding

## Chapter 4 | Results and Discussion

zone. This high temperature results into various types of thermal damage in the form of thermal softening, phase transformation, reduced fatigue strength, cracks and undesirable tensile residual stresses. In conventional grinding, due to very small thermal conductivity of the abrasive grains, the amount of heat carried away via grinding wheel can be neglected.

Grinding zone temperature as estimated for dry and wet grinding under different work velocity and downfeed conditions were reported in Fig.4.4. From the figure, it can be observed that irrespective of grinding condition (dry and wet grinding), increase in downfeed results into gradual increase in temperature which is due to increase in total heat flux ( $q_w$ ) on account of increase in tangential grinding force as per eqn (4.3). Similarly, increase in grinding zone temperature were observed with increase in work velocity which is due to increase in tangential grinding force ( $F_T$ ) with work velocity and the same can be seen from Fig.4.1(a). However, under similar condition, smaller temperature rise is observed under wet grinding as compared to dry grinding due to cooling and lubrication action of cutting fluid.

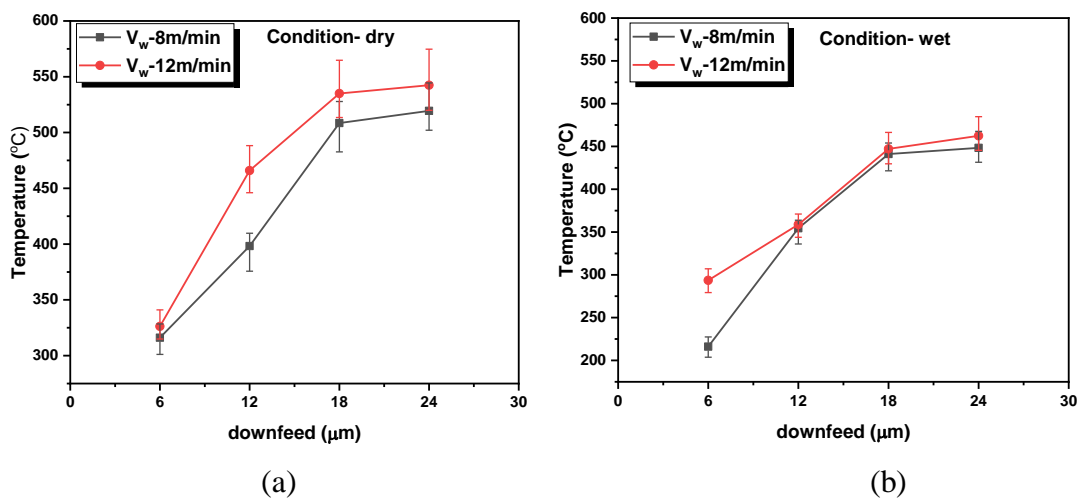


Fig.4.4 Variation of grinding zone temperature with downfeed under different work velocity conditions (a) dry grinding (b) wet grinding

### 4.1.4 Surface Roughness and Topography:

Surface roughness and surface topography assessment plays an important role in evaluating the performance of the ground surface component in real application. The presence of micron size notches on the ground surface leads to localized plastic strain field because of stress concentration at the tip of the notch under the action of applied stress. Thereby, these plastic zones are highly susceptible to stress corrosion and fatigue cracks (Tinnes *et al.*, 2003). Surface roughness in grinding primarily depends on the machinability of the work material, grinding wheel, grinding condition and tribological behavior involved (Davim, 2010). In present investigation, surface roughness of the ground surface is evaluated in terms of arithmetic average surface roughness ( $R_a$ ). In order to improve the repeatability, five such measurement were performed on each sample. The variation in surface roughness against downfeed and work velocity were reported in Fig.4.5 under dry and wet grinding condition. It is evident from the figure that, surface roughness increase with the increase in downfeed and work velocity irrespective of grinding condition (dry and wet grinding). (Charkraborty and Paul, 2008) in their work on numerical modelling of surface topography shows that surface roughness have direct correlation with maximum grit depth of cut. As per eqn (4.1), it can be seen that maximum grit depth of cut increases with increase in downfeed and work velocity. Thereby, a continuous increase in surface roughness is observed with increase in downfeed and work velocity. Additionally, increase in work velocity increases the number of dynamic abrasive grain per unit area and out of which few gets fractured and thus create deeper peak to valley on the ground

## Chapter 4 | Results and Discussion

surface and thus deteriorating the surface finish. Under similar condition, dry grinding results into higher surface roughness as compared to wet grinding, this is due to higher friction and deeper ploughing action causes bulges on both side of the abrasive grit in the absence of cutting fluid between the work surface and randomly oriented abrasive grain. Deeper ploughing creates bulges on both side of the abrasive grit and thus results in poor surface finish

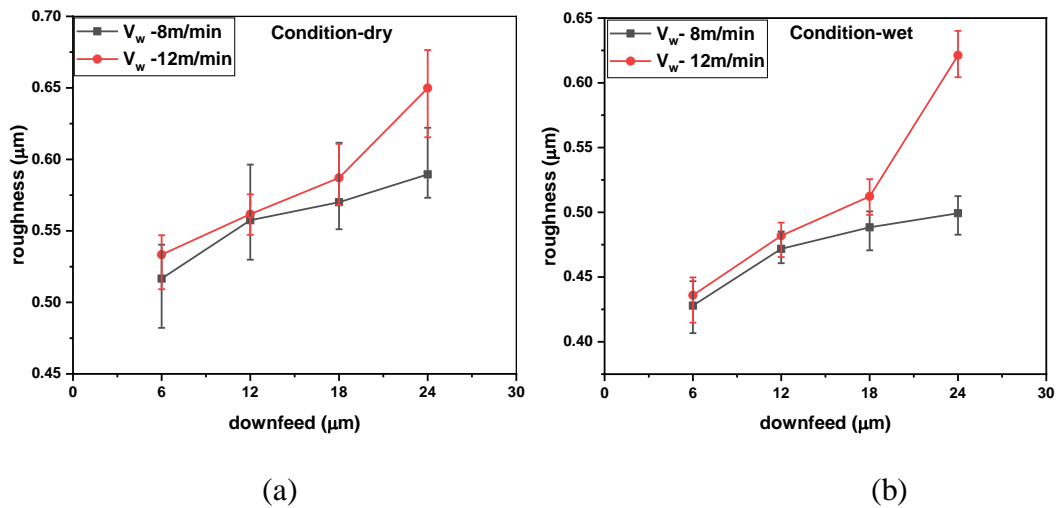


Fig.4.5 Variation of surface roughness with downfeed under different work velocity conditions (a) dry grinding (b) wet grinding

Ground surface topography examines the overlapping scratches generated on account of interaction between abrasive cutting points and work material. Additionally, it helps in predicting the mode of metal removal and the effect of lubricant during abrasive-work material interaction.

Fig.4.6 presents the SEM images (2-D view) of ground surface at highest work velocity for different grinding condition. From the figure, the relative motion of abrasive grit with respect to workpiece can be easily identified from the direction of overlapping scratches and grooves. The sideways propagation of material from the generated scratches owing to ploughing mechanism is also evident.

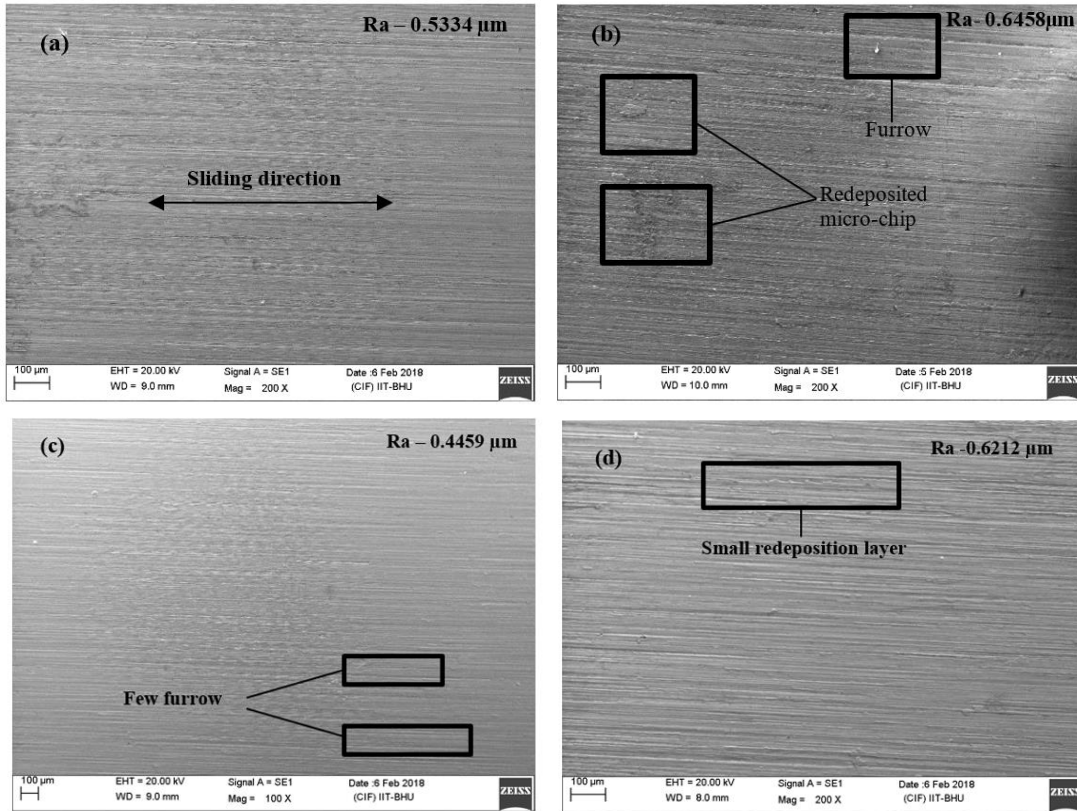


Fig.4.6 SEM images of ground surface for (a) dry grinding, ( $V_w$ -12m/min, downfeed-6 $\mu\text{m}$ ) (b) dry grinding, ( $V_w$ -12m/min, downfeed-24 $\mu\text{m}$ ) (c) wet grinding, ( $V_w$ -12m/min, downfeed-6 $\mu\text{m}$ ) (d) wet grinding, ( $V_w$ -12m/min, downfeed-24 $\mu\text{m}$ ).

A number of large grooves with furrows is observed in dry grinding (refer Fig.4.6 (b)) at higher downfeed. However, under similar condition, wet grinding shows better surface morphology in terms of lesser number of scratches and grooves (refer Fig.4.6 (d)). This is due to the fact that, cutting fluid reduces the grit-workpiece adhesion by lubrication action and thereby reduces the ploughing action.

#### 4.1.5 Metallographic study:

In grinding operation, the combined effect of mechanical and thermal loading, results into various types of surface damage of the ground surface. The extent of mechanical and thermal loading depends on the grinding parameter utilized during the process. The



## Chapter 4 | Results and Discussion

formation of white layer along with phase transformation and grain recrystallization are among the major consequences of such loading conditions. Optical micrographs of subsurface regions obtained from surfaces cut perpendicular to the grinding direction under different grinding conditions are shown in Fig.4.7.

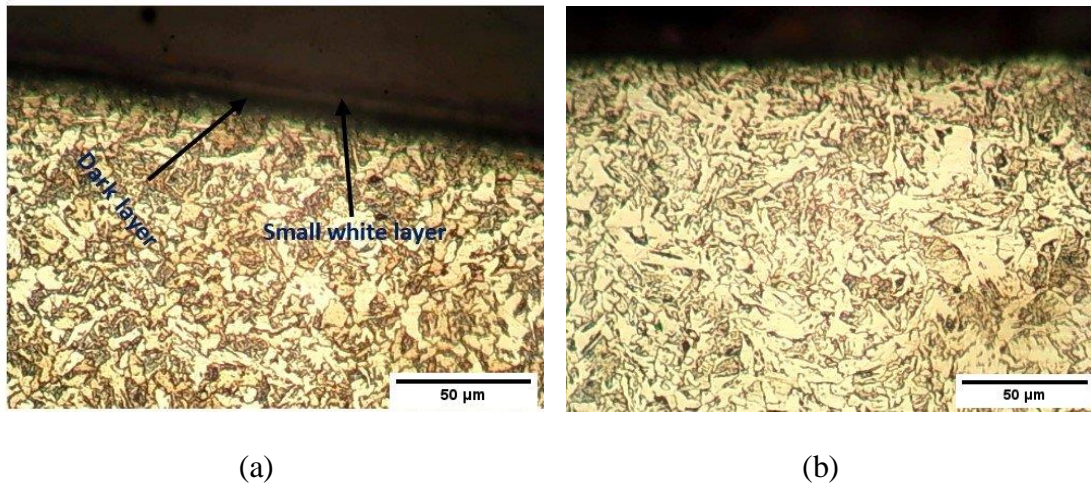


Fig.4.7 Variation in subsurface microstructure of ground sample at 200x and at a downfeed of 24μm and work velocity of 12m/min for (a) dry grinding (b) wet grinding

In the present investigation, a very thin such white layer ( $\sim 5 \mu\text{m}$ ) measured using Image J software is observed as amount of heat and plastic deformation generated during grinding was not enough to cause subsurface alteration in microstructure. A similar observation in microstructure is reported by (Abrao and Aspinwall, 1996; Sosa *et al.*, 2007; Vashista *et al.*, 2009).

### 4.1.6 Microhardness:

The variation in microhardness of the ground surface under different downfeed, work velocity and grinding condition (dry and wet) were reported in Fig.4.8. The measurement were taken just beneath the ground surface and at different location on the same subsurface. High grinding zone temperature followed by rapid cooling

## Chapter 4 | Results and Discussion

induces varying degree of plastic deformation in the subsurface and thereby alters the microhardness of the ground sample. Generally, increased chip thickness and chip load during grinding results into higher plastic deformation on the surface and subsurface causing work hardening (Sosa *et al.*, 2008). This increase in microhardness of the ground surface is undesirable as cracks can easily nucleate and propagate in the hard and brittle surface leading to sudden failure of the ground component. From the figure 4.8 it can be seen that microhardness of ground surface increases with increase in downfeed irrespective of work velocity and grinding condition, this is due to increase in plastic deformation with increase in downfeed. Further, a continuous increase in microhardness is also observed with increase in work velocity as increase in work velocity increases the temperature of the machined surface (refer Fig.4.4) which in turn gives rise to sticking friction between the tool and work material interface and thereby leads to increase in subsurface plastic flow and results into higher microhardness value of the ground surface.

However, under similar grinding condition, microhardness value observed under wet grinding is smaller as compared to those in dry grinding condition. The higher microhardness in case of dry grinding is due to higher grinding zone temperature which in turn produces higher thermal damage in the absence of cutting fluid.

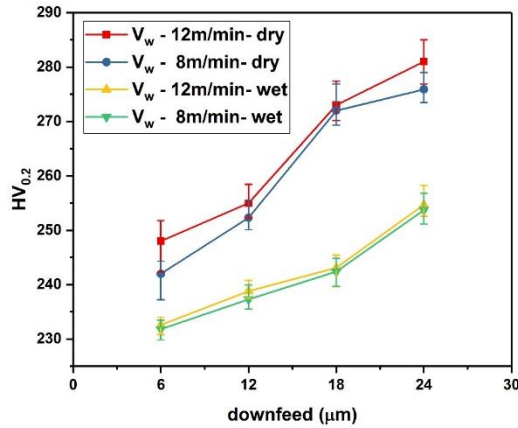


Fig.4.8 Variation of microhardness under different downfeed, work velocity and grinding condition (dry and wet).

Fig.4.9 shows the variation of microhardness value along the depth from the surface. It is clear from the figure that microhardness value just beneath the surface is much higher and as we move along the depth the value goes on decreasing. The maximum percentage change in microhardness (40%) is observed in case of dry grinding at downfeed of 24μm and work velocity of 12m/min with respect to unground sample.

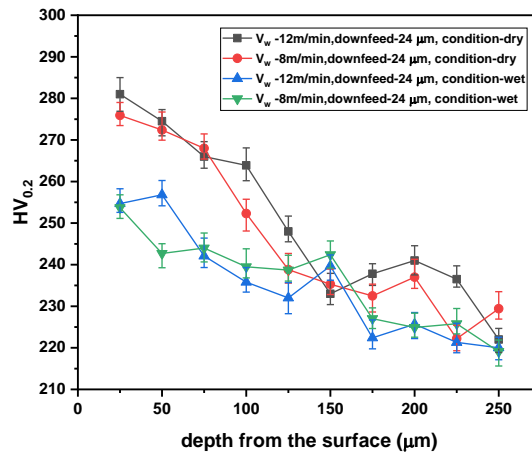


Fig.4.9 Microhardness profile of ground surface along the depth from the surface under different grinding conditions.

## Chapter 4 | Results and Discussion

This is due to the fact that near the surface the cooling rate is much higher which leads to the formation of hard and brittle (untampered martensite) layer whereas in the bulk due to slower cooling rate tempering of martensite results into lower hardness.

### 4.1.7 Residual stress:

Residual stress in grinding is the stress left inside the material, once the external forces (thermal energy or mechanical forces) is removed. In grinding, residual stress generated by mechanical forces is of compressive nature whereas those generated by thermal forces are of tensile nature. Further, as the magnitude of stress generated by thermal forces are higher, the ground surface exhibit a net tensile residual stress. The measurement of these tensile residual stress is important as these reduces the dynamic and static strength of the work material as well as it also reduces the resistance to stress corrosion cracking.

X- ray diffraction technique is a well-established technique which is used to estimate residual stress generated upon grinding. Generally, in this technique, a plot between  $2\theta$  (peak position) against  $\sin^2\Psi$  ( $\Psi$  is the angle subscribed between normal to the surface and the bisector of source and diffracted X-ray beam) were made, and the magnitude of slope of the fitted straight gives the stress value. Gazzara (1983) in his work shows the effect of residual stress on peak position ( $2\theta$ ), in the presence of compressive residual stress the initial position of atom gets reduced which thereby leads to an increase in ( $\theta$ ) in accordance with Bragg's law. Similarly a decrease in ( $\theta$ ) is observed in the presence of tensile residual stress.

Fig.4.10 show the X-ray diffraction profile of ground surface at lowest and highest downfeed for higher work velocity during dry and wet grinding. In this study, the

## Chapter 4 | Results and Discussion

concept of peak shift as discussed earlier were utilized to predict residual stress generated during grinding operation. Fig.4.11 shows the variation in peak shift occur with grinding zone temperature. Peak position of unground sample were taken as reference and thereafter peak position of ground surface were subtracted from the reference to estimate the peak shift. The presence of compressive residual stress

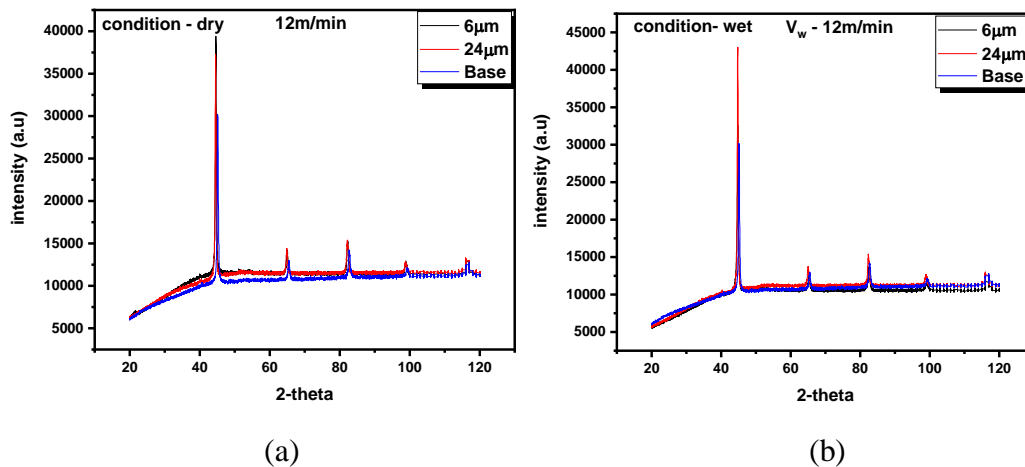


Fig.4.10 X-ray diffraction profile of ground surface at highest work velocity with lowest and highest downfeed condition (a) dry grinding (b) wet grinding

reduces initial position of atom and thereby shift the peak position ( $2\theta$ ) to a higher value in accordance with Bragg's law. However, the presence of tensile residual stress increases the initial position of atom and thereby shift the peak position ( $2\theta$ ) to a lower value. A net reduction in peak position is observed throughout the grinding domain, as reduction in peak position due to presence of tensile residual stress is higher as compared to increase in peak position due to compressive residual stress. A good correlation were observed between peak shift and grinding zone temperature with correlation coefficient of 0.9295.

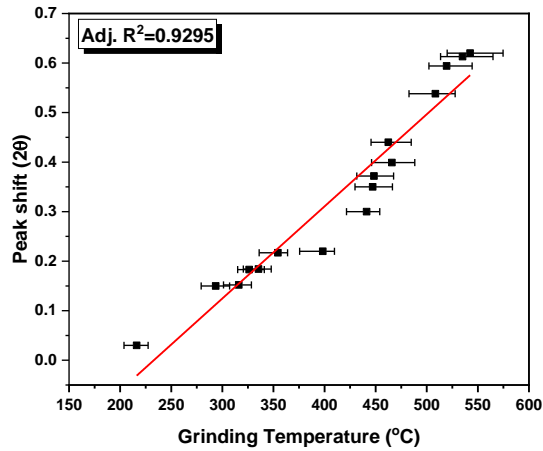


Fig.4.11 Variation in peak shift with grinding zone temperature

#### 4.1.8 Magnetic Barkhausen noise:

In grinding, the process parameter like (work velocity, downfeed and grinding environment) plays a crucial role in the generation of thermal damage to the ground surface. The higher work velocity along with the higher level of applied depth of cut leads to more thermal damage whereas the lower work velocity in combination with lower downfeed produce less severe thermal damage. The presence of thermal damage in the form of grinding burn and residual stresses on the ground surface alters the domain wall motion of the ferromagnetic material under externally applied magnetic field and is therefore have significant influence on the Barkhausen noise emission.

Fig.4.12 shows the effect of grinding process parameter (work velocity, downfeed and grinding environment) on the Barkhausen noise signal. From the figure, it can be seen that magnetic response of the material measured in terms of RMS value of the Barkhausen signal increases with the increases in downfeed and work velocity. This is due to the fact that increasing downfeed and work velocity results in higher rise in grinding zone temperature and thus leading to more thermal damage and consequently

## Chapter 4 | Results and Discussion

increases in BN (RMS) is observed. Further, it is also evident that grinding under dry condition yields higher value of BN (RMS) due to higher thermal load as compared to that of wet grinding.

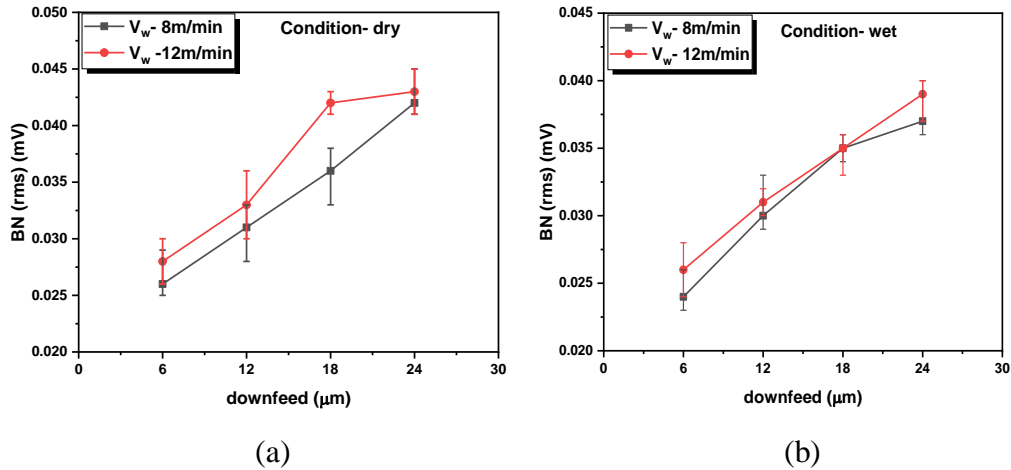


Fig.4.12 Effect of grinding parameter on Barkhausen noise (a) dry grinding (b) wet grinding.

Apart from above, surface roughness of the samples also have significant influence on Barkhausen noise emission. Despite of close contact between magnetic yoke and specimen some sorts of air gap are always present between them and the magnitude of the gap tends to increase with the increases in surface roughness. The presence of larger air gap reduces the effective magnetic permeability which in turn reduces the magnetization and hence Barkhausen noise. The increase in surface roughness result into more spacing between the domain wall and hence its motion becomes rather difficult. Also, with increasing surface roughness more domain walls can be formed through imperfection in the surface which later on can acts as a nucleation center. Fig.4.13 shows the variation in response of the Barkhausen noise with surface roughness of the ground sample in the entire experimental domain. From the figure, it can be evident that, with increases in surface roughness of the sample a continuous

## Chapter 4 | Results and Discussion

increase in BN (RMS) is observed which proves that the surface roughness has significant influence on Barkhausen noise only at higher value of surface roughness and not in the present case as order of surface roughness is very small.

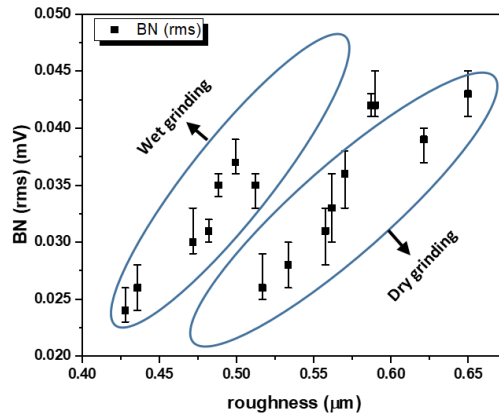


Fig.4.13 Effect of surface roughness on Barkhausen noise

In a ferromagnetic material, under applied external magnetic field, the magnetization takes place due to domain wall motion. The presence of mechanical stresses (residual or applied stresses) alters the arrangement of the domains and the dynamics of the domain walls motion due to magnetoelastic interaction. Thereby, it effects the generated Barkhausen noise signal. This forms the basis of residual stress measurement using magnetic Barkhausen noise technique. Fig.4.14 depicts the variation in Barkhausen noise signal at different level of peak shift. Fig.4.15 clearly shows that as the amount of peak shift increases, there is continuous increase in the root mean square value of the Barkhausen noise signal. As already discussed, larger peak shift corresponds to higher level of tensile residual stress in the sample. Therefore, sample with higher peak shift generates higher amplitude of Barkhausen signal and vice-versa. This is due to the fact that, in material with positive magnetostriction (like steel),



## Chapter 4 | Results and Discussion

presence of tensile residual stress aligns the magnetic domains in a direction parallel to stress direction which in turn favors the magnetization process.

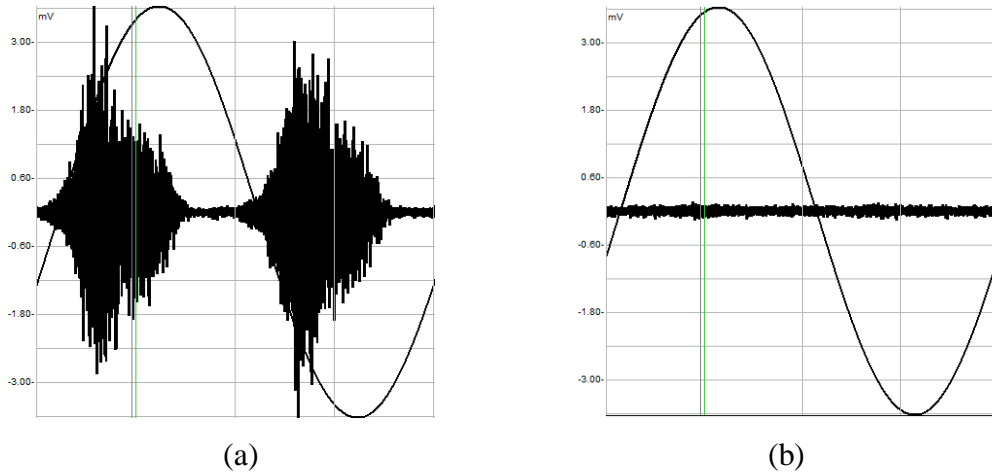


Fig.4.14 Variation in as received Barkhausen noise signal acquired from software for (a) higher peak shift/residual stress (b) lowest peak shift/residual stress conditions.

Similarly, presence of compressive residual stress aligns the magnetic domains in a direction perpendicular to stress direction which in turn makes the magnetization process difficult. Additionally, applied tensile stress reduces the exchange energy, and hence further enhance the Barkhausen jump.

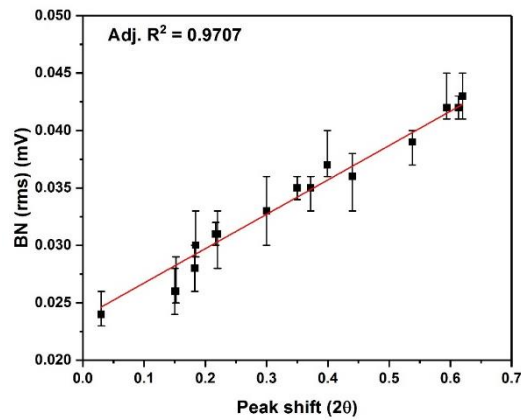


Fig.4.15 Variation in root mean square value of Barkhausen noise signal with peak shift

Further, the linear dependence of Barkhausen noise signal with residual stress is observed with a correlation coefficient  $\sim 0.9707$ . This shows that, the root mean square value of the Barkhausen noise signal can be used to assess the residual stress state of the ground material.

### 4.1.9 Hysteresis loop:

In the previous section, the effect of grinding process parameter on Barkhausen noise has been discussed and it has been shown that grinding parameter plays a major role in defining the extent of thermal damage which in turn affects the micromagnetic response of the material. In the present section effect of grinding variables on the hysteresis loop parameter (average permeability at coercive point) is discussed.

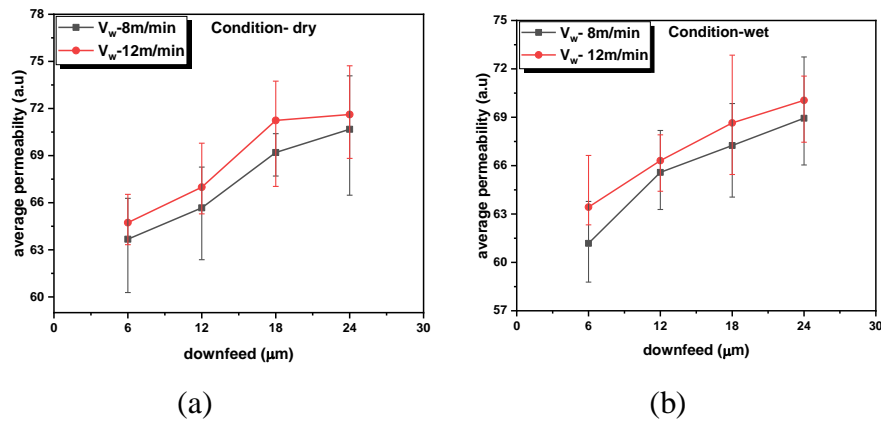


Fig.4.16 Effect of grinding parameter on average permeability (a) dry grinding (b) wet grinding.

Fig.4.16 shows the effect of grinding process parameter (work velocity, downfeed and grinding environment) on the average permeability value. It can be observed that as the case with Barkhausen noise, a similar variation in average permeability value is observed with increase in downfeed and work velocity. This similar behavior of

## Chapter 4 | Results and Discussion

average permeability with process parameter is because of indirect relationship between Barkhausen noise emission and average permeability. The more and more accumulation of thermal damage with increasing downfeed and work velocity result into higher value of average permeability.

Fig.4.17 shows the variation in average permeability with surface roughness of the ground sample in the entire experimental domain. As already discussed that higher surface roughness increases the air gap between which in turn lowers the effective permeability. But, in the grinding process due to very smooth surface finish of the ground surface a firm contact with lower air gap can be established between sensor and specimen. Hence, no decrease in average permeability is observed with increasing surface roughness. This means that effect of surface roughness on average permeability is significant only when surface roughness reached a critical value, at lower value of the surface roughness as in the present case the effects can be neglected.

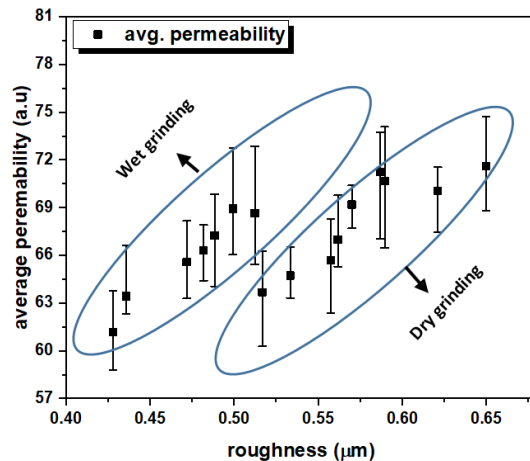


Fig.4.17 Effect of surface roughness on average permeability

Hysteresis loop, a closed curve represents the magnetisation and demagnetisation response of the ferromagnetic material when kept under external magnetic field. The

## Chapter 4 | Results and Discussion

shape and size of the hysteresis loop is greatly influenced by the residual stress state within the material. The presence of residual stress induces stress anisotropy and thereby alters the magnetic permeability which in turn effects the hysteresis loop. Fig.4.18 represents the effect of peak shift on hysteresis loop under different work velocity. The characteristics hysteresis loop of the sample with larger peak shift had lower steepness as compared to the one which has smaller peak shift. Additionally, the distortion in shape of the hysteresis loop were higher at higher work velocity condition as compared to low work velocity. This is because of higher work velocity produces more grinding temperature (refer Fig.4.4) and hence more thermal damage.

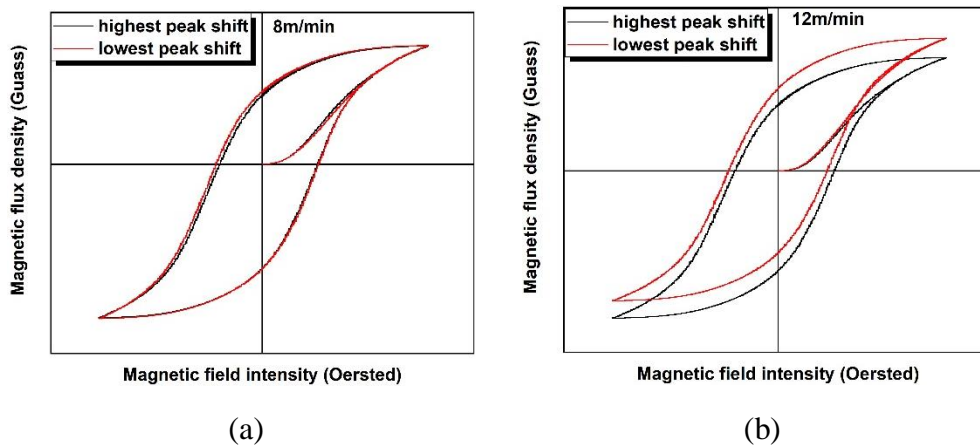


Fig.4.18 Variation in as received hysteresis loop acquire from software for different peak shift condition for different work velocity (a) 8m/min (b) 12m/min

The quantitative characterization of the hysteresis loop were presented in Fig.4.19 in which average permeability derived from the characteristics hysteresis loop were plotted against peak shift derived from X-ray diffraction. From the Figure, it is clear that average permeability increase with the increase in peak shift. The more and more increase in peak shift correspond to more and more induction of tensile residual stress. This tensile residual stress aligns the magnetic domains in a direction parallel to stress

## Chapter 4 | Results and Discussion

direction which in turn favors the magnetization process and hence improves the average permeability. A linear dependence were observed between peak shift and average permeability with a correlation coefficient  $\sim 0.951$ .

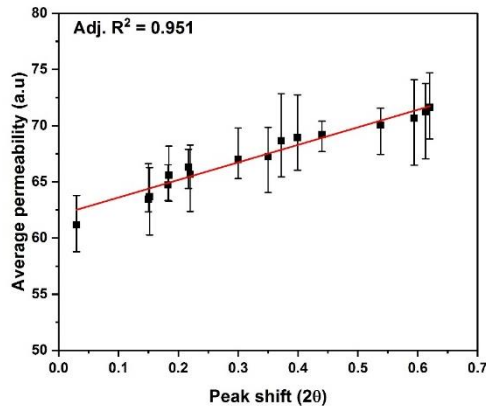


Fig.4.19 Variation in average permeability value derived from hysteresis loop with peak shift

### 4.2 Grinding of hardened (pack carburized) steel:

In present section the grindability of hardened low carbon steel is discussed in terms of grinding forces, specific grinding energy, grinding temperature and surface integrity. The surface integrity measurement includes study of microstructure, microhardness variation, surface roughness and residual stress. Finally, the effect of various process parameter (downfeed, work velocity and grinding condition) and surface integrity on micro magnetic response of the material were discussed in detail.

#### 4.2.1 Grinding forces:

Tangential grinding force which results on account of interaction between abrasive and work material were measured under different downfeed, work velocity and grinding conditions and the resulting variation is reported in Fig.4.20. It can be clearly seen from the figure that with the increase in downfeed from 6  $\mu\text{m}$  to 24  $\mu\text{m}$ , a continuous increase in tangential grinding force is observed. This increase in tangential grinding force with downfeed is due to increase in maximum undeformed chip thickness and also at higher downfeed more number of abrasive grits takes part in the material removal mechanism and thus giving rise to higher force (Li *et al.*, 2006). Apart from above, maximum undeformed chip thickness also increases with the increases in work velocity thereby higher forces is observed at higher work velocity. Grinding environment (dry and wet) also plays a major role in deciding the magnitude of grinding forces. In comparison to wet grinding, higher tangential grinding force is observed during dry grinding when other influential parameter are kept constant. The higher grinding zone temperature during dry grinding generates dulling of the abrasive grit along with its breakage and

## Chapter 4 | Results and Discussion

thus leading to higher grinding forces. Further, in the absence of cutting fluid the chip formed during the shearing action get loaded into the wheel which additionally increases the grinding force.

Under similar condition, the grinding of hardened steel generates lower tangential grinding force as compared to those of unhardened steel. The range of tangential grinding force during grinding of unhardened steel were observed to be in between (16.6 N-70.3 N) whereas those of hardened steel lies in the range (15.3 N- 66.3 N). The material removal by the ploughing mechanism decreases as the hardness of the material to be ground increases hence result into lower grinding force (Garrison and Garriga, 1983).

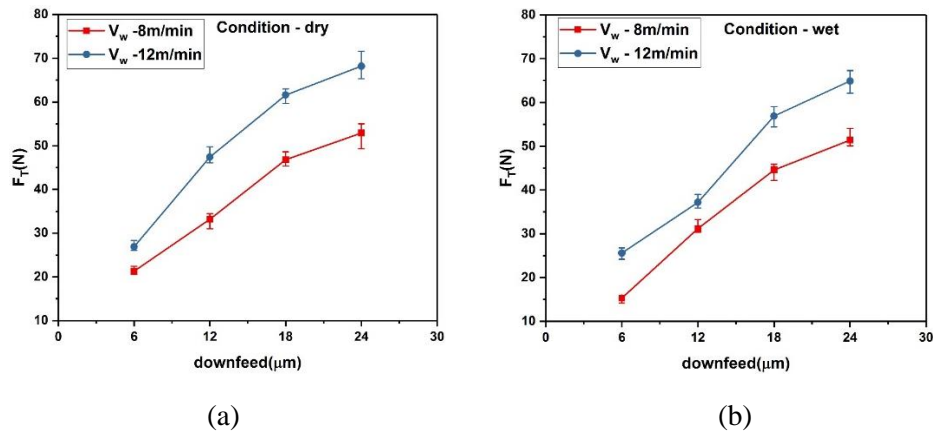


Fig.4.20 Variation in tangential grinding forces with downfeed under different work velocity conditions for (a) dry grinding (b) wet grinding

Fig.4.21 depicts the variation in normal grinding force during grinding of hardened steel under different grinding conditions. Similar to tangential grinding force, normal grinding force also follows the same trend of variation with the downfeed, work velocity and grinding condition. This is because of the fact that as like to tangential grinding force, normal grinding force is also a function of chip load.

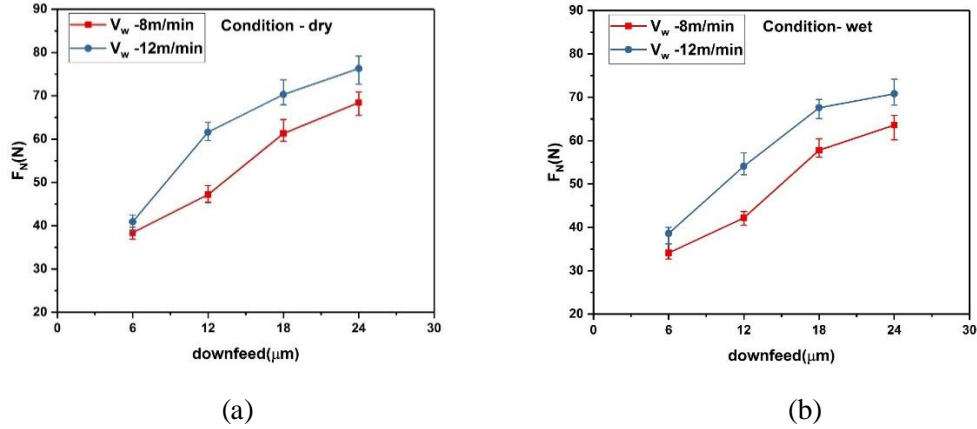


Fig.4.21 Variation in normal grinding forces with downfeed under different work velocity conditions for (a) dry grinding (b) wet grinding

#### 4.2.2 Specific grinding energy:

Fig.4.22 demonstrates the effect of grinding process parameter on specific grinding energy. From the figure, it can be seen that specific grinding energy decreases with the increase in downfeed and work velocity irrespective of grinding conditions (dry and wet). The increase in downfeed and work velocity results into reduction in rubbing and ploughing mechanism along with the reduction in friction between abrasive grit and workpiece and most of the energy supplied is utilized in the desirable shearing action thereby reducing the specific energy (Shenshen et al., 2014). Apart from above ‘size effect’ also contributes significantly in the specific energy requirement. At lower value of downfeed and work velocity there is reduction in the chip thickness causing high dynamic shear strength and hence enhances the energy requirement (Rowe and Chen, 1997). Under identical condition the magnitude of specific grinding energy is higher in dry grinding as compared to that of wet grinding. In the absence of lubrication, dry grinding involves higher friction between abrasive and workpiece leading to higher specific energy.



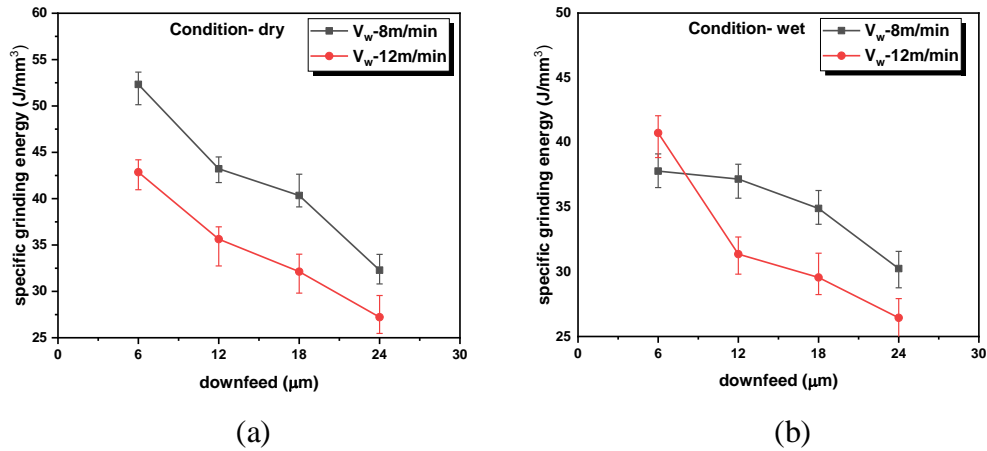


Fig.4.22 Variation in specific grinding energy with downfeed under different work velocity conditions (a) dry grinding (b) wet grinding

### 4.2.3 Grinding temperature:

The variation in temperature during grinding of hardened steel under different condition of process parameter are depicted in Fig.4.23. It is an accepted fact that the, grinding parameter (i.e, downfeed or depth of cut, wheel peripheral speed and table feed or workspeed) have direct effect on the maximum undeformed chip thickness which in turn have significant effect on grinding temperature (Shen *et al.*, 2014; Zhang *et al.*, 2015). It can be seen from the figure that increase in downfeed result into increase in grinding temperature and that too irrespective of grinding environment (dry and wet). The increase in undeformed chip thickness with increase in downfeed result into increases in material removal rates which expectedly increase the grinding temperature. Further, during wet grinding increase in temperature is observed with increase in work velocity whereas during dry grinding the work velocity have reverse effect on the grinding zone temperature as can be seen from Fig.4.23. This decrease in temperature with increase in work velocity during dry grinding may be due to the fact that heat source movement in grinding increases with increasing work velocity which thereby

## Chapter 4 | Results and Discussion

reduces the time that the moving heat source spent with the workpiece and most of the heat generated gets transferred quickly into the atmosphere leading to reduced grinding temperature (Lin *et al.*, 2016).

In addition to the above, grinding environment (dry and wet) also have significant influence on the temperature generated during grinding process. The high specific energy associated with dry grinding result into higher temperature whereas due to effective cooling and lubrication action, wet grinding generates lower temperature.

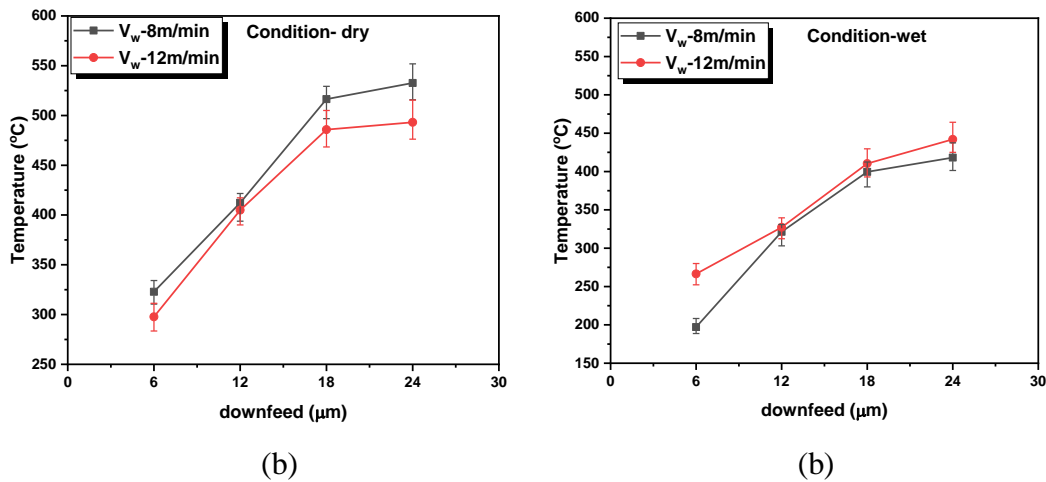


Fig.4.23 Variation of grinding zone temperature with downfeed under different work velocity conditions (a) dry grinding (b) wet grinding

### 4.2.4 Surface Roughness and Topography:

Fig.4.24 depicts the variation in surface roughness during grinding of hardened steel under different downfeed, work velocity and grinding environment. It is evident from the figure that as the downfeed increases there is increase in surface roughness value of the ground surface. Also surface roughness increases with the increase in work velocity. As explained earlier, any combination of parameter which effects the maximum undeformed chip thickness will also have significant effect on the surface

## Chapter 4 | Results and Discussion

roughness. Generally, surface roughness have direct relationship with maximum undeformed chip thickness .The increase in downfeed or work velocity increases the maximum undeformed chip thickness and hence produce more rougher surface. The grinding performed with lubrication also helps in lowering the value of surface roughness and the same can be seen from Fig.4.24. In the presence of lubrication, cleaning of chip occur which would otherwise if left on the surface get stuck to the ground surface during subsequent passes and hence can give rise to higher surface roughness.

It is important to mention that, in comparison to unhardened steel, higher surface finish or lower surface roughness is observed during grinding of hardened steel under identical condition. This is because of the reason that increasing material hardness restrict the formation of bulge on the side edges and hence provides better surface finish (Kitajima *et al.*, 1992).

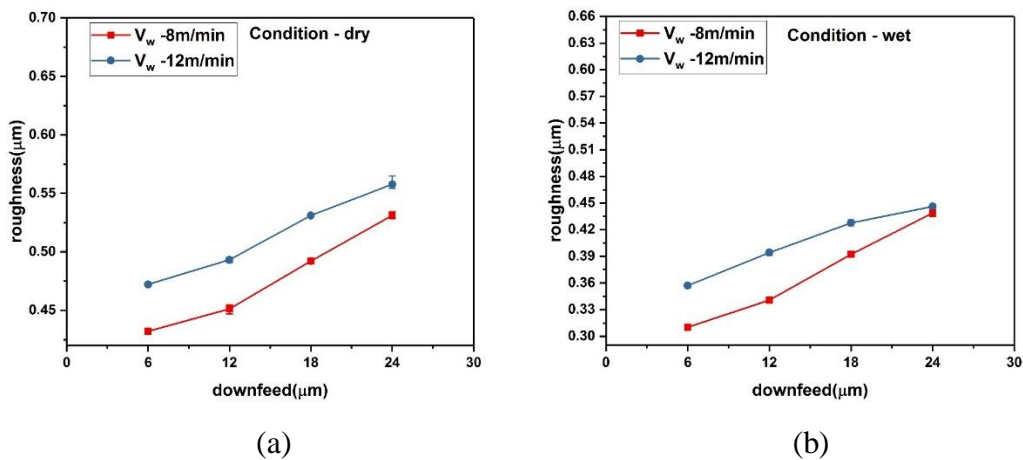


Fig.4.24 Variation of surface roughness with downfeed under different work velocity conditions (a) dry grinding (b) wet grinding

The surface roughness achieved during grinding of unhardened steel were in the range ( $0.4279\mu\text{m}$ - $0.6498\mu\text{m}$ ) whereas those achieved in case of hardened steel were in the

## Chapter 4 | Results and Discussion

range ( $0.3124\mu\text{m}$ - $0.5776\mu\text{m}$ ). The minimum surface roughness were witnessed during wet grinding at lower work velocity and downfeed conditions whereas the higher surface roughness is observed under dry grinding at higher work velocity and downfeed conditions.

The surface morphology of the ground hardened steel at different process parameter conditions are represented in Fig.4.25. The grinding marks as observed in the figure represents the relative motion of grit with respect to workpiece.

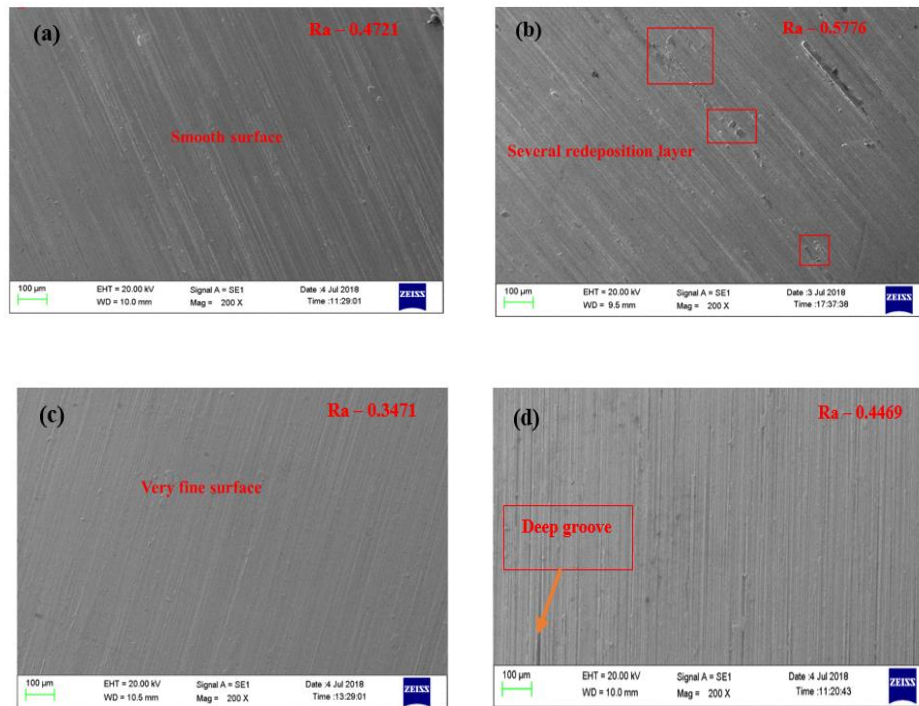


Fig.4.25 SEM images of ground hardened steel for (a) dry grinding, ( $V_w$  - 12 m/min, downfeed -  $6\mu\text{m}$ ) (b) dry grinding, ( $V_w$  - 12 m/min, downfeed -  $24\mu\text{m}$ ) (c) wet grinding, ( $V_w$  - 12 m/min, downfeed -  $6\mu\text{m}$ ) (d) wet grinding, ( $V_w$  - 12 m/min, downfeed -  $24\mu\text{m}$ ).

The smooth surface in terms of lower grooves and lower redeposition of chip can be seen during wet grinding whereas higher surface deterioration was observed during dry grinding. The reason for higher surface roughness in dry grinding can be attributed to

increased ploughing action and higher friction between abrasive grit and workpiece in the absence of lubrication.

### 4.2.5 Metallographic study:

The higher temperature during the grinding is supposed to change the microstructure of the ground surface. The intensity of heat generation in grinding is not only dependent on interaction forces rather it is also significantly influenced by plastic deformation mechanism associated with material removal process, work velocity, and downfeed. Fig.4.26 shows the alteration in subsurface microstructure of the ground surface at highest thermal damage. The higher thermal damage is related to the higher grinding zone temperature which in present case is observed at lower work velocity and higher downfeed during dry grinding whereas in case of wet grinding it is observed at higher work velocity and higher downfeed condition.

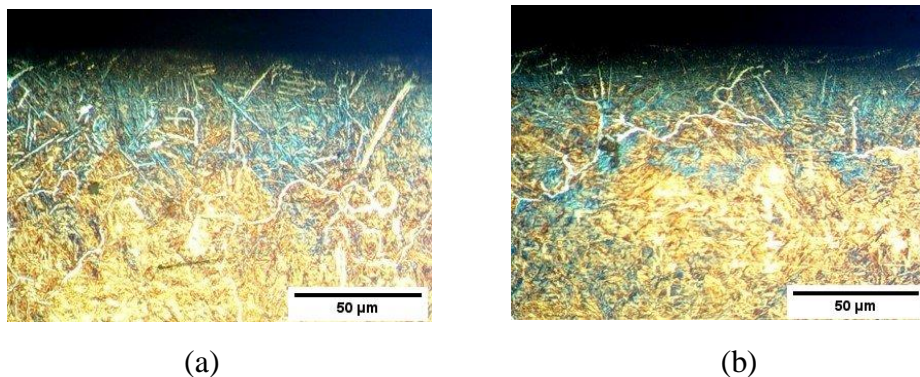


Fig.4.26 Variation in subsurface microstructure of ground sample at 200x for highest thermal damage (a) dry grinding ( $V_w$ -8m/min, downfeed-24  $\mu\text{m}$ ) (b) wet grinding ( $V_w$ -12m/min, downfeed-24  $\mu\text{m}$ )

However, the extent of thermal damage and associated plastic deformation in present observation is not sufficient to cause significant change in the microstructure, thereby

no white layer formation is visible on the ground surface. Similar variation in microstructure is reported by (Silva *et al.*, 2007)

### 4.2.6 Microhardness:

Fig.4.27 report the changes occur in the microhardness value just beneath the ground surface under different work velocity, downfeed and grinding environment. It can be observed from the figure that hardness of the subsurface monotonically increases with the increase in downfeed. This increase in microhardness value with downfeed is due to increase in plastic deformation. Further, in addition to the plastic deformation, phase transformation and grain refinement also causes changes in the hardness value but as the temperature is not sufficient enough to cause phase transformation changes mainly occur due to plastic deformation (Eda *et al.*, 1993; Sosa *et al.*, 2007). Along with the downfeed, work velocity also have significant contribution on microhardness value. As reported earlier that lower velocity in comparison to higher velocity in case of dry grinding result into higher temperature generation, thereby causing more tempering of the martensite in the hardened steel as it already contains martensite during carburizing process and hence shows lower hardness value.

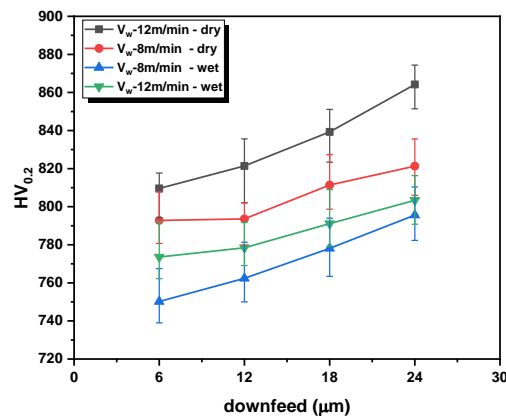


Fig.4.27 Variation of microhardness under different downfeed, work velocity and grinding condition (dry and wet).

## Chapter 4 | Results and Discussion

The variation in microhardness value as a function of depth from the ground surface for different grinding condition is depicted in Fig.4.28. The gradual decrease in hardness value is observed as the depth from the ground surface increases. As at lower downfeed the changes occurred in hardness value is not appreciable thereby there is no question of gradual decrease hence is not shown.

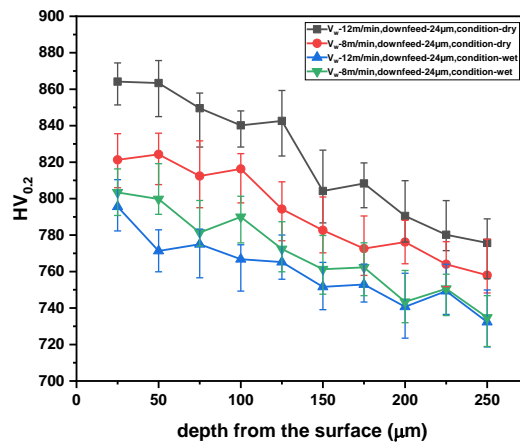


Fig.4.28 Microhardness profile of ground surface along the depth from the surface under different grinding conditions.

### 4.2.7 Residual stress:

The X-ray diffraction profile of ground hardened steel under different grinding process parameter conditions are shown in Fig.4.29. As already stated that shift in peak position can be used as a measure to quantify state of residual stress, a rightward peak shift (towards higher peak position) relative to the reference sample shows the presence of compressive residual stress whereas leftward peak shift (towards lower peak position) relative to the reference sample shows the presence of tensile residual stress.

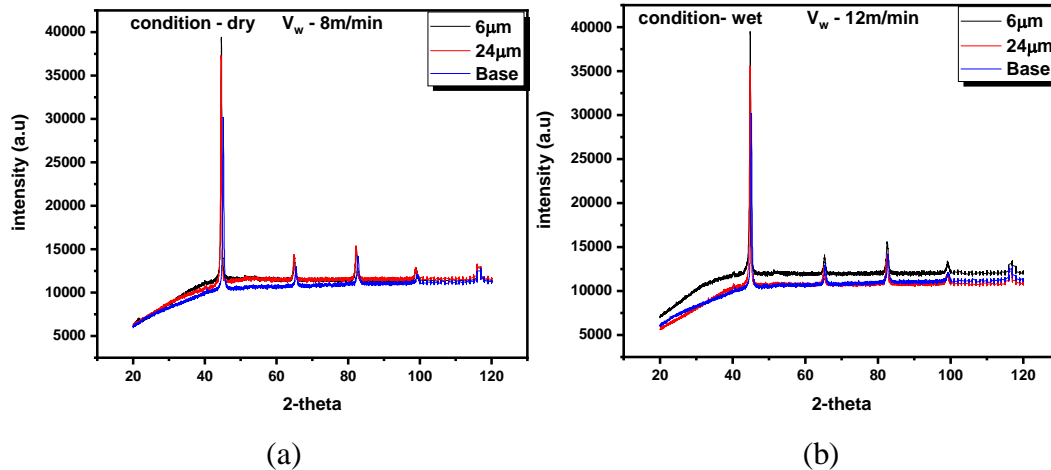


Fig.4.29 X-ray diffraction profile of ground hardened surface (a) dry grinding (b) wet grinding

The peak shift is computed for the entire set of ground hardened steel by taking peak position of unground hardened steel as a reference. In present study a continuous peak shift towards left of the reference peak position is observed which indicates the presence of tensile residual stress. Further, higher tensile residual stress on account of higher thermal damage shows more shift in peak position. Fig.4.30 shows the variation of peak shift with grinding temperature in the complete experimental domain. A good correlation were observed between peak shift and grinding zone temperature with correlation coefficient of 0.920.

In comparison to ground unhardened steel lower order of peak shift is observed during grinding of hardened steel. The peak shift during conventional grinding of unhardened steel were in the range (0.03-0.62) whereas those in case of hardened steel it lies in the range (0.010-0.412). This lower order of peak shift in hardened steel in comparison to unhardened steel is due to lower thermal damage on account of lower grinding zone temperature.



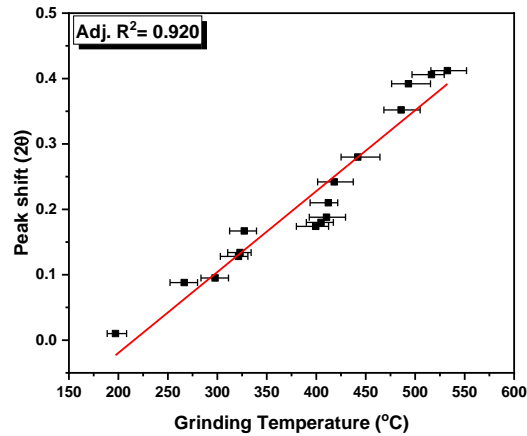


Fig.4.30 Variation in peak shift with grinding zone temperature for hardened steel

### 4.2.8 Magnetic Barkhausen noise:

As per the discussion made in the section (4.1.8) it has been seen that thermal damage in grinding have significant influence on the micromagnetic property of the ground specimen. This change in magnetic property on the other hand have considerable effect on the Barkhausen emission. It has been shown that higher thermal damage induces higher order of tensile residual stress on the ground surface which in turn alters the domain structure in such a way that it increases the Barkhausen noise signal. However, it is important to be mentioned that magnetization response of unhardened steel is much higher as compared to that of hardened steel. Thereby, it is important to see the sensitivity of Barkhausen noise signal towards thermal damage occurring on the surface of ground hardened steel. Fig.4.31 demonstrate the effect of grinding process parameter on Barkhausen noise emission.

From the figure, it can be seen that magnetic response of the material measured in terms of RMS value of the Barkhausen signal increases with the increase in downfeed irrespective of work velocity and grinding environment. The is due to the reason that

## Chapter 4 | Results and Discussion

increase in downfeed increases the grinding zone temperature causing more thermal damage (specifically tensile residual stress) and thereby leading to rise in the Barkhausen noise emission. Further, in comparison to dry grinding lower thermal damage taking place in case of wet grinding and hence reduces the Barkhausen noise emission.

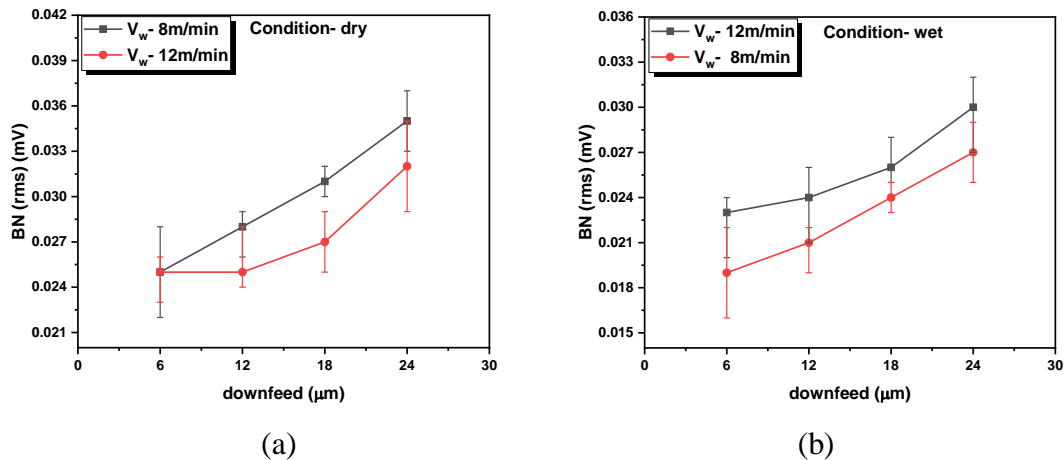


Fig.4.31 Effect of grinding parameter on Barkhausen noise (a) dry grinding (b) wet grinding.

Surface roughness of the ground surface also have their contribution in the Barkhausen noise emission. The presence of air gap between the magnetic yoke (pick up coil) and specimen tends to increase with the increase in surface roughness which reduces the effective magnetic permeability and hence effect the Barkhausen noise emission. But, the effect of surface roughness on Barkhausen noise is supposed to be considered only for the surface having larger surface roughness as smaller surface roughness did not have significant influence on Barkhausen emission. Further, as the surface roughness observed in the case of ground hardened steel is much smaller than those of ground unhardened steel and hence its effect on Barkhausen noise is not discussed.

## Chapter 4 | Results and Discussion

Fig.4.32 depicts the correlation between peak shift due to induction of tensile residual stress with the associated Barkhausen noise. It can be observed that response of Barkhausen noise towards peak shift is not linear rather it follows a polynomial variation. However, in case of ground unhardened steel a linear variation was observed between the Barkhausen noise and peak shift. The reason for the above can be given to poor magnetization of the hardened steel. The increase in hardness is supposed to increase the pinning strength causing difficulty in the motion of domain wall which reduces the magnetization of the material. The response of Barkhausen noise emission from hardened non ground specimen is shown in Fig.4.33.

Even though the response of Barkhausen noise towards peak shift is not linear but increase in peak shift tends to increase the Barkhausen noise emission and is evident from the Fig.4.32. As already discussed, the increase in peak shift represents the more and more induction of tensile residual stress which in turn aligns the magnetic domains in a direction parallel to stress direction and hence enhances the Barkhausen jumps.

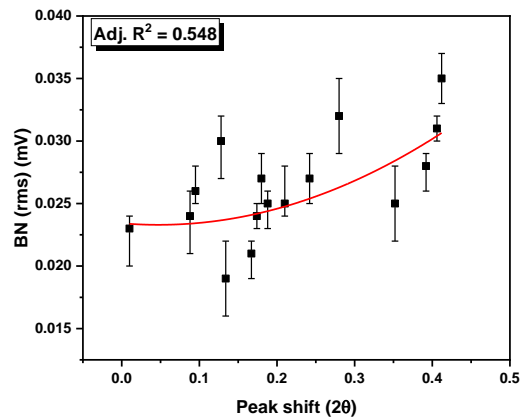


Fig.4.32 Variation in root mean square value of Barkhausen noise signal with peak shift for ground hardened steel.

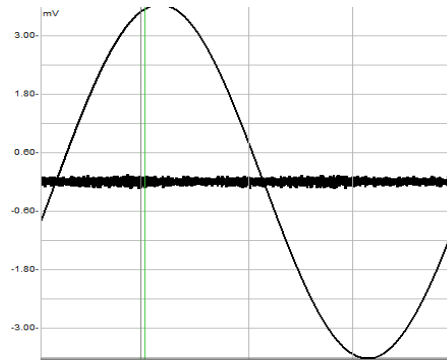


Fig.4.33 A snapshot showing the Barkhausen noise signal obtained from hardened steel.

### 4.2.9 Hysteresis loop:

It has been seen previously that process parameter during the grinding operation controls the temperature rise and thereby also have significant influence on the level of thermal damage which in turn effect the magnetic response of the material. Fig.4.34 depicts the effect of grinding process parameter namely downfeed, work velocity and grinding environment on the magnetic parameter (average permeability). From the figure it can be observed that during dry grinding increase in downfeed and reduction in work velocity increases the average permeability whereas during wet grinding average permeability value increases with the increase in downfeed and work velocity. Further, lower average permeability value is observed in wet grinding as compared to dry grinding and is because of lower temperature rise associated with wet grinding.

In case of unhardened steel the average permeability value lies in the range (63.68-71.62) for dry grinding condition whereas for those during wet grinding it lies in the range (61.18-70.05). However, in case of hardened steel average permeability value lies in the range (57.30-60.21) for dry grinding whereas for those during wet grinding it lies in the range (50.13-55.90). In addition to thermal damage, higher hardness of the material also have pronounced effect on the magnetic response of the material. Increase

## Chapter 4 | Results and Discussion

in hardness of the material result into increase in pinning sites (dislocation density) which restrict the motion of domain wall and thereby reduces the magnetic response.

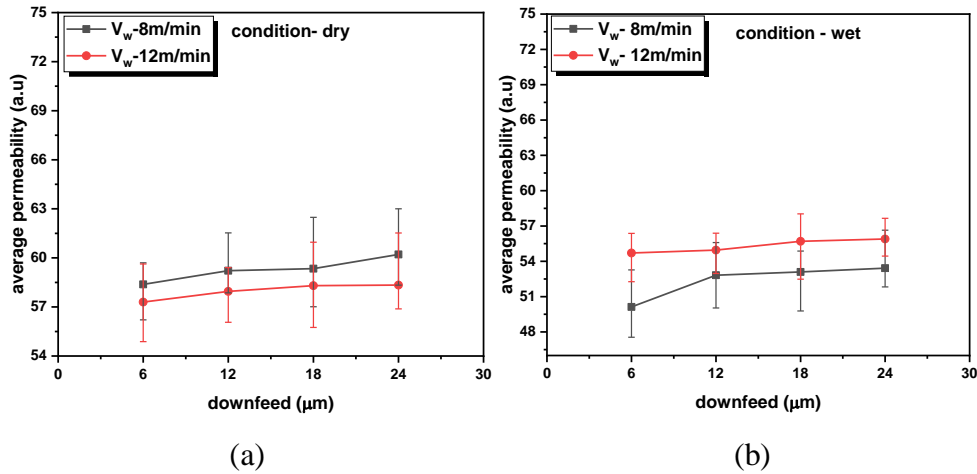


Fig.4.34 Effect of grinding parameter on average permeability for hardened steel (a) dry grinding (b) wet grinding.

In an attempt to investigate the effect of residual stress on the average permeability value, it is important to see the influence of surface roughness on the magnetic behavior of the material. However, it has been already discussed that at lower value of surface roughness as observed in the case of hardened steel which is far below as compared to those observed in unhardened steel, the effect of surface roughness can be ignored hence is not shown.

Fig.4.35 represents the correlation between average permeability and peak shift derived from X-ray diffraction for the entire experimental domain during grinding of hardened steel. Despite of poor magnetic response due to higher hardness, a linear correlation can be observed between the peak shift and average permeability value with a correlation coefficient of  $\sim 0.8149$ . It can be seen from the figure that higher peak shift

## Chapter 4 | Results and Discussion

leads to higher average permeability and the reason for such behavior is very similar to as discussed earlier.

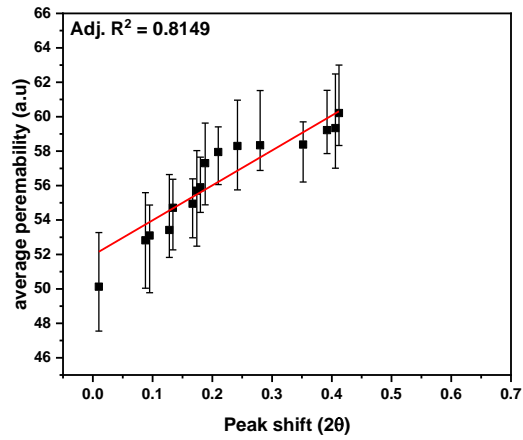


Fig.4.35 Variation in average permeability value derived from hysteresis loop with peak shift during grinding of hardened steel